ChemComm

COMMUNICATION

View Article Online
View Journal | View Issue

Cite this: *Chem. Commun.*, 2023, 59, 1153

Received 9th December 2022,
Accepted 3rd January 2023

DOI: 10.1039/d2cc06705f

rsc.li/chemcomm

Enantioselective reductive allylic alkylation enabled by dual photoredox/palladium catalysis†

Sheng Tang,[a] Hong-Hao Zhang*[ab] and Shouyun Yu *[a]

A dual photoredox/palladium catalyzed regio- and enantioselective reductive cross-coupling of allylic acetates with tertiary/secondary alkyl bromides has been achieved, and Hantzsch ester is used as a homogeneous organic reductant. This straightforward protocol enables the stereoselective construction of C(sp^3)–C(sp^3) bonds under mild reaction conditions. Mechanistic studies suggest that this reaction involves radical pathways and a chiral Pd complex enables the control of the regio- and enantioselectivities.

Over the past decades, transition metal-catalyzed reductive cross-coupling reactions have emerged as one of the most powerful and straightforward protocols to construct carbon–carbon bonds efficiently.[1] This procedure eliminates the need for preformed organometallic reagents in conventional transition metal-catalyzed cross-coupling reactions[2] by coupling two electrophiles directly in the presence of a terminal reductant. Enantioselectivity remains a significant challenge in this field.[3] While considerable efforts have been devoted during the last decade, asymmetric reductive cross-coupling reactions are mainly focused on C(sp^2)–C(sp^3) couplings (Scheme 1(a), top).[3] The development of enantioselective reductive C(sp^3)–C(sp^3) cross-couplings has been hampered historically by deleterious side-reactions, such as β-H elimination or homocoupling of C(sp^3)-electrophiles (Scheme 1(a), bottom).[4–6] This is particularly true for the sterically hindered C(sp^3) electrophiles, such as tertiary alkyl halides. To meet these challenges, novel reductive and catalytic systems would be highly desirable.[7]

Metallaphotoredox catalysis, the merger of photoredox catalysis with transition metal catalysis, has received considerable attention recently.[8] It has been applied to the area of reductive reactions, enabling the coupling of electrophiles with homogeneous organic reductants under mild conditions.[9] Despite advances, enantioselective versions of metallaphotoredox-catalyzed reductive couplings are still limited.[10,11] We recently achieved a photoredox/Pd-cocatalyzed regio-, diastereo-, and enantioselective reductive homocoupling of allylic acetates (Scheme 1(b)).[12] Encouraged by the success of the allylic-allylic homocoupling, as well as our lasting research interest in enantioselective palladium metallaphotoredox catalysis,[13] we aim to realize the enantioselective reductive C(sp^3)–C(sp^3) cross-coupling of allylic acetates with tertiary alkyl halides using this state of the art synthetic technology (Scheme 1(c)).

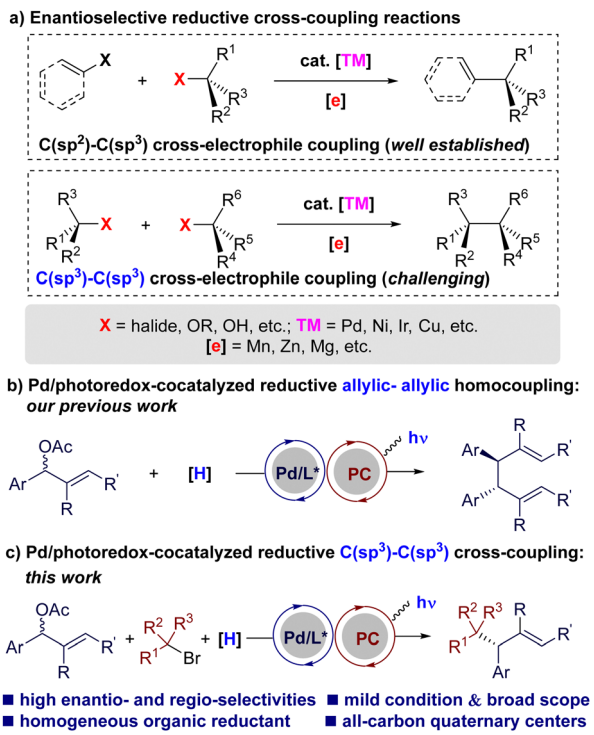

Scheme 1 Enantioselective reductive cross-coupling reactions.

[a] State Key Laboratory of Analytical Chemistry for Life Science, Jiangsu Key Laboratory of Advanced Organic Materials, Chemistry and Biomedicine Innovation Centre (ChemBIC), School of Chemistry and Chemical Engineering, Nanjing University, Nanjing 210023, China. E-mail: yushouyun@nju.edu.cn
[b] School of Petrochemical Engineering, Changzhou University, Changzhou 213164, China. E-mail: zhanghonghao@cczu.edu.cn

† Electronic supplementary information (ESI) available. See DOI: https://doi.org/10.1039/d2cc06705f

Table 1 Reaction condition optimization[a]

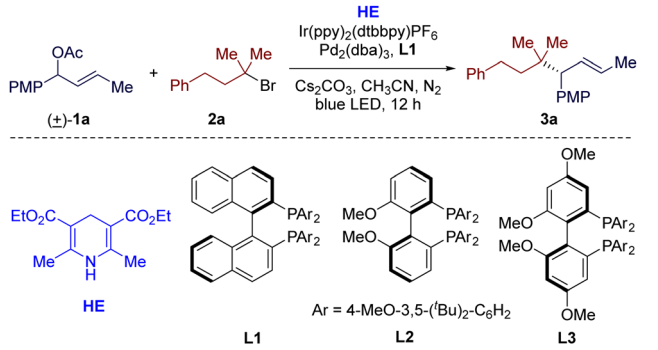

Entry	Variation of reaction conditions	Yield[b]/%	ee[c]/%	rr[b]
1	None	75[d] (70)	96	>95:5
2	**L2** instead of **L1**	40	98	94:6
3	**L3** instead of **L1**	36	98	95:5
4	*fac*-Ir(ppy)$_3$	0	—	—
5	Ir(dFCF$_3$ppy)$_2$(dtbbpy)PF$_6$	0	—	—
6	w/o HE	0	—	—
7	DIPEA in instead of HE	44	92	92:8
8	TEA in instead of HE	35	94	92:8
9	CH$_3$CN (2 mL) was used	67	96	>95:5
10	w/o light or Ir(ppy)$_2$(dtbbpy)PF$_6$	0	—	—
11	w/o Pd$_2$(dba)$_3$ or **L1**	0	—	—

[a] Reaction conditions: a solution of **1a** (0.1 mmol), **2a** (0.3 mmol), **HE** (0.2 mmol), Cs$_2$CO$_3$ (0.2 mmol), Pd$_2$(dba)$_3$ (2.5 mol%), ligand (6 mol%), and Ir(ppy)$_2$(dtbbpy)PF$_6$ (2 mol%) in CH$_3$CN (4.0 mL) was irradiated by a 45 W blue LED for 12 h. [b] Yields and regiomeric ratios (rr) were determined by GC analysis. [c] Enantiomeric excess (ee) values were determined by HPLC on a chiral stationary phase. [d] Isolated yield. PMP = *para*-methoxyphenyl. DIPEA = diisopropylethylamine. TEA = triethylamine.

We began our investigations into this reductive cross-coupling protocol using racemic allylic acetate **1a** and tertiary alkyl bromide **2a** as the model substrates. After a comprehensive evaluation of the reaction parameters (see ESI† for details), the optimal conditions were established. When a solution of **1a** (1.0 equiv.), **2a** (3.0 equiv.), Hantzsch ester (**HE**, 2.0 equiv.) and Cs$_2$CO$_3$ (2.0 equiv.) in CH$_3$CN was irradiated by a 45 W blue LED at room temperature for 12 h in the presence of photocatalyst Ir(ppy)$_2$(dtbbpy)PF$_6$ (2 mol%) and Pd$_2$(dba)$_3$ (2.5 mol%)/(*R*)-DTBM-BINAP (**L1**, 6 mol%) (Table 1, entry 1), the reductive cross-coupling reaction was achieved and the desired product (**3a**) was afforded in a good yield (75% GC yield and 70% isolated yield) and excellent regio- and enantioselectivities (>95:5 rr, 96% ee). Replacing the chiral diphosphine ligand **L1** with MeO-BIPHEP (**L2**) or GARPHOS (**L3**), the optimal ligands of our previous allylic alkylation reactions,[12,13] also resulted in excellent regio- and enantioselectivities, but significantly lower yields due to serious homocoupling of allylic acetate **1a** (entries 2 and 3). Several other iridium-based photocatalysts, such as *fac*-Ir(ppy)$_3$ and Ir(dFCF$_3$ppy)$_2$(dtbbpy)PF$_6$, were employed, but were not superior to Ir(ppy)$_2$(dtbbpy)PF$_6$ (entries 4 and 5). No reaction occurred in the absence of reductant **HE** (entry 5). The choice of homogeneous organic reductants also turned out to be crucial for this transformation, as replacing **HE** with DIPEA or TEA led to a significant drop in the yield (entries 7 and 8). The increase of concentration had negative effects on yield of this reaction (entry 9). Control experiments verified the necessity of visible light and a photocatalyst (entry 10). The palladium catalyst and the chiral ligand were also essential to this reaction (entry 11).

With the optimal conditions in hand, we investigated the scope and limitations of this dual photoredox/Pd-catalyzed enantioselective reductive cross-coupling. As shown in Scheme 2(a), the disubstituted allylic acetates **1** were first examined. Under the standard conditions, various allylic acetates **1** were alkylated with tertiary alkyl bromide s(**2a** or **2b**), offering the corresponding cross-coupling products **3a–3l** in moderate to high yields (34–70%), good enantioselectivities (64–96% ee), and excellent regioselectivities (>95:5 rr). Electron-donating or electron-withdrawing substituents at different positions of the phenyl moiety were all tolerated in this reaction. In comparison, substrates with electron-donating groups could give higher yields (**3a** *vs.* **3d** and **3e**). Polycyclic aromatic allylic acetate **1g** was also applicable for this reaction, but with poor yield. Besides methyl, the alkyl group of the allylic acetates could be ethyl (**3h**), propyl (**3i**), and even longer pentyl (**3j**)

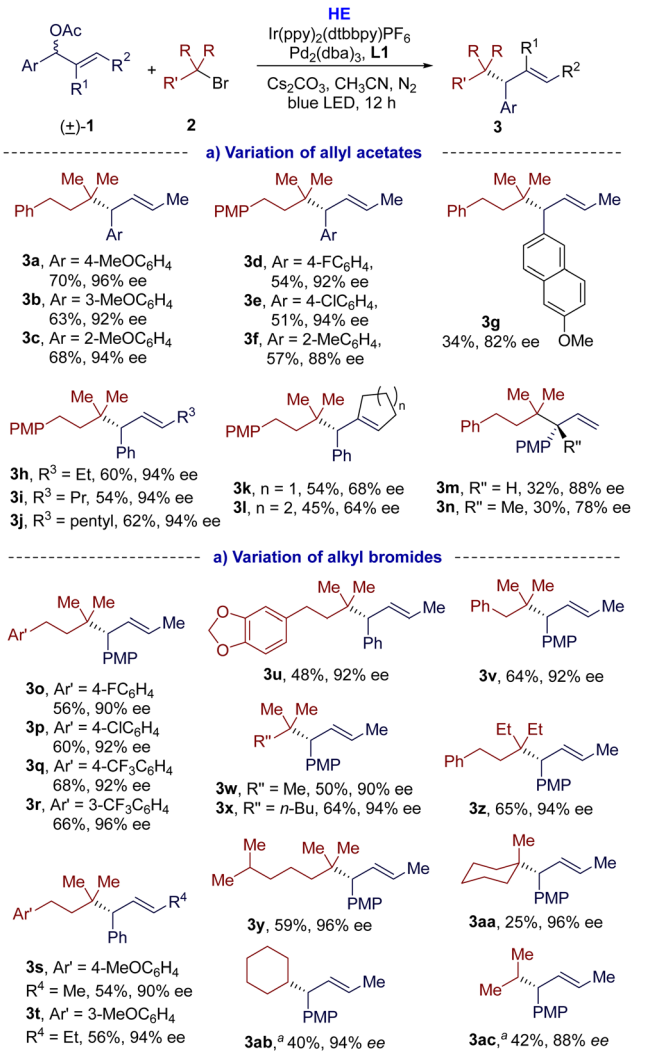

Scheme 2 Substrate scope and limitation. [a]The reaction was run at 0 °C.

groups. Cyclic allyl acetates could also be applicable to this transformation and provided the corresponding products **3k** and **3l** in moderate yields (54% and 45% yield, respectively) and enantioselectivities (68% and 64% ee, respectively). When monosubstituted allyl acetate **1m** was alkylated with **2a** under the established conditions, the desired product **3m** was obtained (32% yield and 88% ee), together with significant homocoupling and over-reduction side products, which could be responsible for the poor yield. Allylic *gem*-alkyl, aryl-disubstituted acetate **1n** was also applicable, affording the desired product **3n** with all-carbon quaternary stereogenic centres with good enantioselectivity (78% ee) and 30% yield. We next investigated the scope of tertiary alkyl bromides. As indicated in Scheme 2(b), this protocol was amenable to tertiary alkyl bromides with phenyl groups bearing either electron-donating or electron-withdrawing substituents at different positions, affording the desired cross-coupling products (**3o–3v**) in 48–68% yields and with excellent enantio- and regioselectivities (90–96% ee, >95 : 5 rr). Non-aryl substituted tertiary alkyl bromides were compatible with the coupling conditions to give the desired products **3w–3y** with moderate yields (50–64%) and good enantioselectivities (90–96% ee). The allylic acetate could be alkylated with the bulkier tertiary alkyl bromide **2m** to give **3z**. Cyclic tertiary bromides also undertook this transformation, but the yield of **3aa** was only 25%. The reductive cross-coupling products with secondary alkyl bromides were also feasible, but at a lower temperature (0 °C). The desired reductive cross-coupling products **3ab** and **3ac** were obtained in moderate yields (40% and 42%, respectively), and excellent regio- and enantioselectivities (>95 : 5 rr, 94% and 88% ee, respectively). All attempts to couple with primary bromides failed (for more details, see Fig. S7 in ESI†).

To gain additional insight into the reaction, we performed several control experiments. Under the standard conditions, allyl acetates **1o**, **1o′** (isomer of **1o**), and an equimolar mixture of them gave similar results, respectively (Scheme 3(a), eqn (1)). When optically pure allyl acetate (*S*)-**1o′** was used as a substrate, the stereochemistry of the product is controlled by the chiral ligand (Scheme 3(a), eqn (2)). These results demonstrate that this reaction goes through a π-allylpalladium intermediate. When the radical trapping reagent TEMPO was introduced to the reaction mixture, the desired reaction could be terminated completely and the TEMPO-trapped product **4** could be observed by high-resolution mass spectrometric analysis (Scheme 3(a), eqn (3)). These phenomena, together with the results of the control experiments in Table 1 (entry 10), suggest that this reaction undergoes a photoredox catalysis process and an alkyl radical might be its key intermediate. Stern–Volmer quenching experiments indicate that the excited photocatalyst is quenched by **HE** (Fig. S5 in ESI†).

Based on these results and previously published works on photoredox/Pd co-catalysis,[12–14] a plausible mechanism is proposed (Scheme 3(b)). An excited-state photocatalyst Ir(III)* is formed by the absorption of visible light, which is reductively quenched by **HE** to give a low-valent Ir(II) complex. Oxidative addition of alkyl bromide **2** to Pd(0) gives alkyl-Pd(II) species **A**. The β-H elimination side product of **A** could be detected by

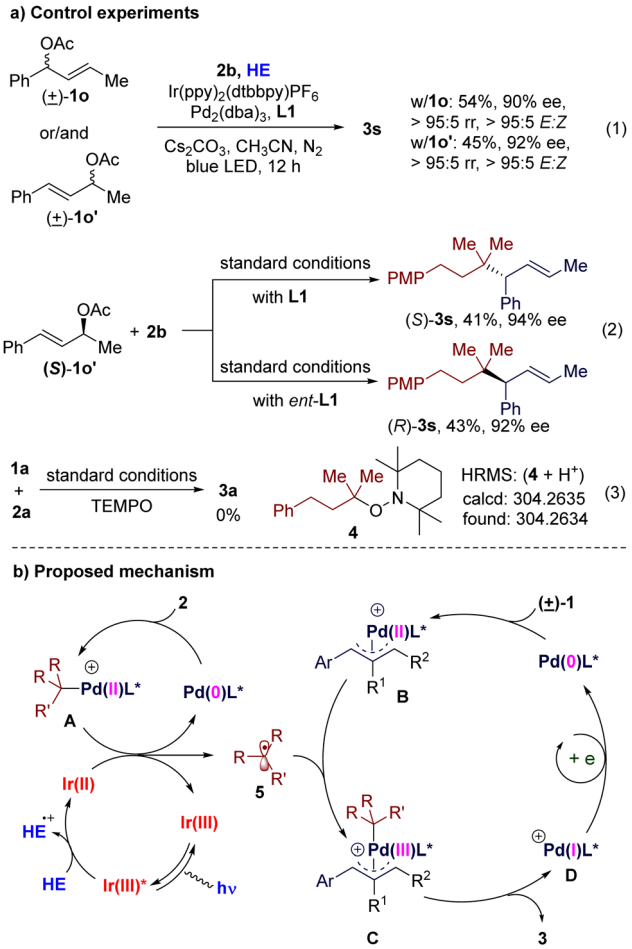

Scheme 3 Mechanism studies and proposal.

GC-MS, which supports the existence of **A**. Reduction of **A** by the Ir(II) complex regenerates Ir(III) and Pd(0), together with an alkyl radical **5**. Meanwhile, Pd(0) oxidatively adds to the allylic acetate **1** to give a Pd-π-allyl species **B**. Then **B** traps the alkyl radical **5** to generate the Pd(III) complex **C**. Reductive elimination of **C** gives the allylic alkylation product **3** and a Pd(I) species **D**. Finally single-electron reduction of **D** by the Ir(II) complex or the **HE** radical cation regenerates Pd(0). Alternatively, an excited-state palladium catalysis pathway cannot be ruled out completely at this stage (for more detailed discussions, see Fig. S6 in ESI†).[15] However, the necessity of a photocatalyst suggests that the cooperative photoredox and palladium catalysis pathway might be the major route.

In summary, we have described a highly regio- and enantioselective reductive C(sp^3)–C(sp^3) cross-coupling of allylic acetates with tertiary/secondary alkyl bromides through cooperative palladium and photoredox catalysis, and Hantzsch ester is used as the reductant. This dual catalytic protocol allows a direct and stereoselective construction of C(sp^3)–C(sp^3) bonds enantioselectively. This mechanistically novel strategy expands the scope of the traditional transition metal-catalyzed asymmetric allylic alkylation reactions and enantioselective reductive cross-coupling reactions.

We thank the National Natural Science Foundation of China (21971110, 21732003, and 22001120), and the Natural Science Foundation of Jiangsu Province (BK20200297) for financial support.

Conflicts of interest

There are no conflicts to declare.

Notes and references

1 For selected reviews on reductive couplings, see: (*a*) C. E. I. Knappke, S. Grupe, D. Gärtner, M. Corpet, C. Gosmini and A. Jacobi von Wangelin, *Chem. – Eur. J.*, 2014, **20**, 6828–6842; (*b*) T. Moragas, A. Correa and R. Martin, *Chem. – Eur. J.*, 2014, **20**, 8242–8258; (*c*) D. J. Weix, *Acc. Chem. Res.*, 2015, **48**, 1767–1775; (*d*) J. Gu, X. Wang, W. Xue and H. Gong, *Org. Chem. Front.*, 2015, **2**, 1411–1421; (*e*) X. Wang, Y. Dai and H. Gong, *Top. Curr. Chem.*, 2016, **374**, 43; (*f*) X. Pang, P.-F. Su and X.-Z. Shu, *Acc. Chem. Res.*, 2022, **55**, 2491–2509; (*g*) M. J. Goldfogel, L. Huang and D. J. Weix, *Nickel Catalysis in Organic Synthesis*, 2020, pp.183–222.

2 For selected reviews on conventional transition metal-catalyzed cross-coupling reactions, see: (*a*) M. R. Netherton and G. C. Fu, *Adv. Synth. Catal.*, 2004, **346**, 1525–1532; (*b*) R. Jana, T. P. Pathak and M. S. Sigman, *Chem. Rev.*, 2011, **111**, 1417–1492; (*c*) A. H. Cherney, N. T. Kadunce and S. E. Reisman, *Chem. Rev.*, 2015, **115**, 9587–9652.

3 For selected reviews on stereoselective reductive couplings, see: (*a*) E. L. Lucas and E. R. Jarvo, *Nat. Rev. Chem.*, 2017, **1**, 0065; (*b*) K. E. Poremba, S. E. Dibrell and S. E. Reisman, *ACS Catal.*, 2020, **10**, 8237–8246.

4 For selected reviews on $C(sp^3)$–$C(sp^3)$ couplings, see: (*a*) A. C. Frisch and M. Beller, *Angew. Chem., Int. Ed.*, 2005, **44**, 674–688; (*b*) F. Glorius, *Angew. Chem., Int. Ed.*, 2008, **47**, 8347–8349; (*c*) A. Rudolph and M. Lautens, *Angew. Chem., Int. Ed.*, 2009, **48**, 2656–2670; (*d*) X. Hu, *Chem. Sci.*, 2011, **2**, 1867–1886; (*e*) J. Choi and G. C. Fu, *Science*, 2017, **356**, eaaf7230.

5 For selected examples of reductive $C(sp^3)$–$C(sp^3)$ cross-couplings, see: (*a*) X. Qian, A. Auffrant, A. Felouat and C. Gosmini, *Angew. Chem., Int. Ed.*, 2011, **50**, 10402–10405; (*b*) Y. Dai, F. Wu, Z. Zang, H. You and H. Gong, *Chem. – Eur. J.*, 2012, **18**, 808–812; (*c*) H. Xu, C. Zhao, Q. Qian, W. Deng and H. Gong, *Chem. Sci.*, 2013, **4**, 4022–4029; (*d*) J.-H. Liu, C.-T. Yang, X.-Y. Lu, Z.-Q. Zhang, L. Xu, M. Cui, X. Lu, B. Xiao, Y. Fu and L. Liu, *Chem. – Eur. J.*, 2014, **20**, 15334–15338; (*e*) H. Chen, X. Jia, Y. Yu, Q. Qian and H. Gong, *Angew. Chem., Int. Ed.*, 2017, **56**, 13103–13106; (*f*) A. B. Sanford, T. A. Thane, T. M. McGinnis, P.-P. Chen, X. Hong and E. R. Jarvo, *J. Am. Chem. Soc.*, 2020, **142**, 5017–5023.

6 For selected examples of stereoselective reductive $C(sp^3)$–$C(sp^3)$ cross-couplings, see: (*a*) E. J. Tollefson, L. W. Erickson and E. R. Jarvo, *J. Am. Chem. Soc.*, 2015, **137**, 9760–9763; (*b*) L. W. Erickson, E. L. Lucas, E. J. Tollefson and E. R. Jarvo, *J. Am. Chem. Soc.*, 2016, **138**, 14006–14011; (*c*) H. Fu, J. Cao, T. Qiao, Y. Qi, S. J. Charnock, S. Garfinkle and T. K. Hyster, *Nature*, 2022, **610**, 302–307.

7 For selected examples of reductive cross-couplings with tertiary alkyl halides, see: (*a*) C. Zhao, X. Jia, X. Wang and H. Gong, *J. Am. Chem. Soc.*, 2014, **136**, 17645–17651; (*b*) X. Wang, S. Wang, W. Xue and H. Gong, *J. Am. Chem. Soc.*, 2015, **137**, 11562–11565; (*c*) X. Wang, G. Ma, Y. Peng, C. E. Pitsch, B. J. Moll, T. D. Ly, X. Wang and H. Gong, *J. Am. Chem. Soc.*, 2018, **140**, 14490–14497.

8 For selected reviews on metallaphotoredox catalysis, see: (*a*) K. L. Skubi, T. R. Blum and T. P. Yoon, *Chem. Rev.*, 2016, **116**, 10035–10074; (*b*) J. C. Tellis, C. B. Kelly, D. N. Primer, M. Jouffroy, N. R. Patel and G. A. Molander, *Acc. Chem. Res.*, 2016, **49**, 1429–1439; (*c*) A. Y. Chan, I. B. Perry, N. B. Bissonnette, B. F. Buksh, G. A. Edwards, L. I. Frye, O. L. Garry, M. N. Lavagnino, B. X. Li, Y. Liang, E. Mao, A. Millet, J. V. Oakley, N. L. Reed, H. A. Sakai, C. P. Seath and D. W. C. MacMillan, *Chem. Rev.*, 2022, **122**, 1485–1542.

9 For selected examples of metallaphotoredox-catalyzed reductive couplings, see: (*a*) Z. Duan, W. Li and A. Lei, *Org. Lett.*, 2016, **18**, 4012–4015; (*b*) P. Zhang, C. C. Le and D. W. C. MacMillan, *J. Am. Chem. Soc.*, 2016, **138**, 8084–8087; (*c*) R. T. Smith, X. Zhang, J. A. Rincón, J. Agejas, C. Mateos, M. Barberis, S. García-Cerrada, O. de Frutos and D. W. C. MacMillan, *J. Am. Chem. Soc.*, 2018, **140**, 17433–17438; (*d*) F. Song, F. Wang, L. Guo, X. Feng, Y. Zhang and L. Chu, *Angew. Chem., Int. Ed.*, 2020, **59**, 177–181; (*e*) T. J. Steiman, J. Liu, A. Mengiste and A. G. Doyle, *J. Am. Chem. Soc.*, 2020, **142**, 7598–7605.

10 For selected reviews on the enantioselective metallaphotoredox catalysis, see: (*a*) H.-H. Zhang, H. Chen, C. Zhu and S. Yu, *Sci. China: Chem.*, 2020, **63**, 637–647; (*b*) A. Lipp, S. O. Badir and G. A. Molander, *Angew. Chem., Int. Ed.*, 2021, **60**, 1714–1726; (*c*) F.-D. Lu, J. Chen, X. Jiang, J.-R. Chen, L.-Q. Lu and W.-J. Xiao, *Chem. Soc. Rev.*, 2021, **50**, 12808–12827.

11 For selected examples of metallaphotoredox-catalyzed enantioselective reductive couplings, see (*a*) H. Guan, Q. Zhang, P. J. Walsh and J. Mao, *Angew. Chem., Int. Ed.*, 2020, **59**, 5172–5177; (*b*) S. H. Lau, M. A. Borden, T. J. Steiman, L. S. Wang, M. Parasram and A. G. Doyle, *J. Am. Chem. Soc.*, 2021, **143**, 15873–15881; (*c*) P. Zheng, P. Zhou, D. Wang, W. Xu, H. Wang and T. Xu, *Nat. Commun.*, 2021, **12**, 1646; (*d*) H. Wang, P. Zheng, X. Wu, Y. Li and T. Xu, *J. Am. Chem. Soc.*, 2022, **144**, 3989–3997.

12 H.-H. Zhang, M. Tang, J.-J. Zhao, C. Song and S. Yu, *J. Am. Chem. Soc.*, 2021, **143**, 12836–12846.

13 (*a*) H.-H. Zhang, J.-J. Zhao and S. Yu, *J. Am. Chem. Soc.*, 2018, **140**, 16914–16919; (*b*) H.-H. Zhang, J.-J. Zhao and S. Yu, *ACS Catal.*, 2020, **10**, 4710–4716; (*c*) X. Shen, L. Qian and S. Yu, *Sci. China: Chem.*, 2020, **63**, 687–691; (*d*) C. Song, H.-H. Zhang and S. Yu, *ACS Catal.*, 2022, **12**, 1428–1432; (*e*) X. Bai, L. Qian, H.-H. Zhang and S. Yu, *Org. Lett.*, 2021, **23**, 8322–8326.

14 For selected examples of photoredox/Pd co-catalysis, see: (*a*) D. Kalyani, K. B. McMurtrey, S. R. Neufeldt and M. S. Sanford, *J. Am. Chem. Soc.*, 2011, **133**, 18566–18569; (*b*) S. B. Lang, K. M. O'Nele and J. A. Tunge, *J. Am. Chem. Soc.*, 2014, **136**, 13606–13609; (*c*) J. Xuan, T.-T. Zeng, Z.-J. Feng, Q.-H. Deng, J.-R. Chen, L.-Q. Lu, W.-J. Xiao and H. Alper, *Angew. Chem., Int. Ed.*, 2015, **54**, 1625–1628; (*d*) C. Zhou, P. Li, X. Zhu and L. Wang, *Org. Lett.*, 2015, **17**, 6198–6201; (*e*) K. Shimomaki, K. Murata, R. Martin and N. Iwasawa, *J. Am. Chem. Soc.*, 2017, **139**, 9467–9470; (*f*) J. Zheng, A. Nikbakht and B. Breit, *ACS Catal.*, 2021, **11**, 3343–3350.

15 For selected reviews on excited-state palladium catalysis, see: (*a*) P. Chuentragool, D. Kurandina and V. Gevorgyan, *Angew. Chem., Int. Ed.*, 2019, **58**, 11586–11598; (*b*) W.-M. Cheng and R. Shang, *ACS Catal.*, 2020, **10**, 9170–9196; (*c*) K. P. S. Cheung, S. Sarkar and V. Gevorgyan, *Chem. Rev.*, 2022, **122**, 1543–1625.

